Potential modulation by strain in lateral surface superlattices

A. R. Long,* E. Skuras, and S. Vallis
Department of Physics and Astronomy, Glasgow University, Glasgow, G12 8QQ, United Kingdom

Ramon Cuscó
Institut Jaume Almera, Consell Superior d'Investigacions Científiques (CSIC), Lluís Solé i Sabarís s.n., 08028 Barcelona, Spain

Ivan A. Larkin,† John H. Davies, and M. C. Holland
Department of Electronics and Electrical Engineering, Glasgow University, Glasgow, G12 8QQ, United Kingdom
(Received 29 October 1998)

We have measured the magnitude of the potential modulation below gated one-dimensional lateral surface superlattices fabricated with periods between 60 and 600 nm on a range of GaAs/AlGaAs heterostructures. The magnitude of the modulation was obtained by studying the amplitude of the commensurability oscillations in magnetoresistance, and confirmed by analysis of the low field positive magnetoresistance step. Without gate bias applied, the modulation is generated by strain in the gates, coupled piezoelectrically to the two-dimensional electron gas. Both magnitude and harmonic content of the potential are in reasonable agreement with a recent theoretical calculation of this coupling, over the full range of periods and for all the structures studied. Away from zero gate bias electrostatic modulation adds to the piezoelectric component. This differs according to the sign of the applied bias. In depletion it increases roughly linearly with bias and is in good agreement with theoretical estimates, whereas in positive bias it tends to saturate as strong screening in the donor layers develops. [S0163-1829(99)01927-X]

I. INTRODUCTION

Electrons moving in a two-dimensional electron gas (2DEG) in a modulation-doped heterostructure have large mean free paths and hence it is possible to perform experiments in which this mean free path is greater than 1 or more critical dimensions of a device.[1] An early experiment of this type was the study of the magnetoresistance due to a periodic modulation of the 2DEG resulting from either an array of metallic gates deposited on the surface of the heterostructure across the direction of current flow or a periodic optical excitation. The result in both cases was a series of magnetoresistance oscillations driven by commensurability between the period of the modulation and the cyclotron radius.[2–4] We refer to these oscillations as commensurability oscillations (COs). Early theoretical analyses related the magnitude, frequency, and phase of the COs to the amplitude and period of the potential modulation induced by the gates.[4–6] In a further study of gated superlattices, Beton *et al.*[7,8] explained the low field positive magnetoresistance (PMR) step that generally accompanies the COs. They ascribed this structure to the effect of open orbits running along the equipotentials in the 2DEG, and estimated the field of maximum resistance and the magnitude of the effect.

In the case of a metallic gated sample, the obvious source of the periodic modulation is a potential difference between the gate elements and the semiconductor surface in between. In a number of recent experiments,[9,10] which used lateral surface superlattices (LSSLs) on particularly shallow 2DEGs, we showed that there was a periodic potential even when the gates were grounded. There was also a strong second harmonic component in the COs. In a previous paper,[11] we considered possible sources of this modulation. We were unable to reproduce the harmonic content of the measured potential assuming a built-in voltage on the gates which would generate the modulation electrostatically. Instead we proposed that differential contraction between the gate and semiconductor led to strain which caused the observed modulation of the 2DEG. It is now recognized[12] that strain plays a role in many experiments where electronic transport is sensitive to weak potentials.

We assumed in our first calculation[11] that strain coupled to the 2DEG through the deformation potential. This gave good qualitative agreement with experiment and explained the strong second harmonic observed. However, the predicted potential modulation was too small by nearly an order of magnitude when all sources of screening were taken into account, including the effect of a parasitic layer of electrons around the donors in the experimental structure. In III-V semiconductors, strain also couples to electrons through the piezoelectric effect. This interaction depends on orientation, unlike the deformation potential. Most samples are grown on (100) surfaces and we assumed in our initial analysis that current flowed along the [010] direction. There is no piezoelectric interaction in this case. However, practical devices, including those fabricated by Cuscó *et al.*[9,10] are usually oriented parallel to the {011} cleavage planes, and current flows along a ⟨011⟩ direction. This maximizes the piezoelectric coupling and the potentials we initially calculated are therefore incomplete for most experiments. In a further theoretical paper[13] we have calculated the piezoelectric interaction and shown that it is of the correct magnitude to explain the data of Cuscó *et al.*[9] We have also exploited in a recent experiment[14] the angular dependence predicted for the piezoelectric coupling in order to confirm that this interaction is indeed dominant. In this experiment we fabricated superlat-

tices at different angles to the crystallographic axes, and backed off the strain induced modulation with an electrostatic potential on the gates. We thereby showed that the piezoelectric coupling is of opposite sign for current flowing in the [011] and [01$\bar{1}$] directions as is predicted by the theory.

The main aims of this paper are to report an extended study of the variations of the amplitude of the COs for LSSLs fabricated on different types of heterostructure and with a wide range of periods, and to compare these observations with the predictions of the piezoelectric model for zero gate bias and with the electrostatic models at finite gate bias. Specifically, we intend the following.

(i) To describe the magnitudes and harmonic contents of the potential modulations observed for a wide range of different samples fabricated on GaAs/AlGaAs and GaAs/AlAs heterostructures with the 2DEG confined at different distances from the surface.

(ii) To compare the magnitudes of the potential modulation deduced from the amplitudes of the COs and from the low field positive magnetoresistance structure.

(iii) To show how the elastic and the electrostatic contributions to the modulation interact together, and to compare the magnitudes observed with the theoretical predictions in Davies *et al.*[11] and Larkin *et al.*[13]

In the next section we discuss the layer structures, fabrication processes and measurement techniques used. This is followed by a critical account of how modulation amplitudes may best be deduced from experimental data. We discuss the magnitude of the modulation observed without any voltage applied to the gates, which is caused predominantly by strain. The harmonic content in the COs gives important information about the source of the modulation and we discuss this in detail. Finally we look at the effect of varying gate bias in both positive and negative directions.

II. EXPERIMENTAL TECHNIQUES

A. Sample requirements

The first requirement for our samples is that the perturbation induced by the gates should be passed to the underlying 2DEG without excessive attenuation. The theoretical work suggests that both electrostatic effects and the results of the strain are proportional to $\exp(-2\pi nz/L)$, where z is the coordinate into the semiconductor from the surface, L is the period of the superlattice, and n is the harmonic number of the perturbation. Hence for low attenuation we require a large ratio of L/d, where d is the depth of the 2DEG. In this work we used samples with L/d ratios between 2 and 20. At the lower bound of this range, higher harmonics particularly are strongly attenuated.

Our second requirement is that the electron mean free path in the 2DEG should be sufficiently large that electrons are able to describe cyclotron orbits without significant scattering. In the simplest models for COs,[4–6] this means that the transport mean free path should be greater than the cyclotron orbit circumference commensurate with the fundamental period of the superlattice ($l \gg \pi L$), which with superlattices of periods around 200 nm (a typical value) and standard 2DEG materials is relatively easy to satisfy. However, recent studies[15,16] have pointed out that small angle scattering can disproportionately attenuate the COs. As for a typical 2DEG the quantum or unweighted mean free path (l_q), which does not deemphasise small angle scattering, can be a factor of ten or more less than the transport mean free path, the condition ($l_q \gg \pi L$) is a much more restrictive one. Particularly in reverse gate bias, this can significantly affect the observed amplitudes of the COs. We discuss this point in more detail in Sec. III A below.

One of the features of the data we are strongly interested in is the harmonic content of the COs. It is well known[10] that if a superlattice is fabricated with a mark/space ratio different from unity, then a second harmonic in the potential and the resulting COs naturally results. This conclusion is supported by our theoretical analyses.[11,13] Therefore in order to investigate the harmonic structure introduced by strain perturbation, we have restricted ourselves in this study to superlattices in which the gate widths are nominally equal to their separations, a mark/space ratio of 1. The effect of small lithographic errors on the mark/space ratio and hence on the magnitude of any second harmonic component in the COs will be discussed in the relevant section.

B. 2DEG structures

For the original work on short period superlattices (and also on other nanoelectronic devices), we developed[17] shallow δ-doped heterostructures with the electrons confined against interfaces 28 nm from the surface, and with spacer thicknesses of 11 nm. Those with this geometry and AlGaAs barriers generally were found to have too low a mobility to be suitable for these studies, but equivalent layers with AlAs barriers were used for much of the earlier work.[9,10] In these layers, a sheet of mobile electrons round the donors screens the random potential and raises the mobility to values approaching 100 $m^2\,V^{-1}\,s^{-1}$.[17] We call this layer structure ''type 1.'' For the work on the orientational dependence of the piezoelectric interaction,[14] we used δ-doped AlGaAs barrier material with a 20 nm spacer, in which the electrons were trapped against an interface 38 nm from the surface. Typical electron mobilities for this layer were around 40 $m^2\,V^{-1}\,s^{-1}$ (type 2). Experiments were also performed using standard slab-doped deep 2DEGs with the electrons 92 nm from the surface, which have mobilities in excess of 100 $m^2\,V^{-1}\,s^{-1}$ (type 3). Experiments using all three layer types are described in this paper. The mobility values we have quoted are for samples cooled slowly and measured in the dark, our normal experimental conditions.

C. Fabrication and measurement

The LSSLs were fabricated on wet etched Hall bars with channel widths between 10 and 100 μm. The superlattices were fabricated across the Hall bars using electron beam lithography, positive resist and lift off, with generally 50 to 100 periods. Using this technique periods down to 60 nm were fabricated. Even at this short period, the behavior of the superlattices was semiclassical and dominated by the COs. To make reliable electrical contact to all the superlattice fingers on deep material, it was generally found necessary to bring the gate pads over the etched edges of the Hall bars. The voltage leads on the Hall bars were close to the superlattice but outside it. Inevitably this produced resistance in

series with that of the superlattice itself, which was subtracted from the data as necessary.

Samples were measured either at 1.4 or 4.2 K to suppress the Shubnikov–de Haas oscillations, using a standard low frequency lock-in amplifier technique. The low field magnetoresistance was generally measured at a range of positive and negative gate voltages, and with no gate voltage applied.

III. DEDUCING MODULATION POTENTIALS FROM THE MAGNETORESISTANCE DATA

We have used in the main two features for deducing modulation amplitudes from the magnetoresistance traces, the COs themselves and the positive magnetoresistance step. We discuss the interpretation of these in turn. One other phenomenon in the magnetoresistance which reflects the magnitude of the periodic potential has also recently been observed. Geim *et al.*[18] have shown that above the highest field CO, a quadratic component in the magnetoresistance is sometimes found. This behavior is implicit in the semiclassical model[5] and its magnitude can in principle be used to estimate the periodic potential. However, we do not find this phenomenon to be universal in our data; it occurs for long period superlattices measured at high temperatures on low mobility material, where the Shubnikov–de Haas oscillations do not overlap the COs. For most of our samples, these oscillations interfere and the quadratic magnetoresistance is either greatly weakened or not seen. We do not therefore discuss it further here.

A. Potentials from the CO amplitudes

To interpret the COs we use the semiclassical expression derived for a simple sinusoidal modulation by Beenakker[5] and developed for higher harmonics by Gerhardts.[6] This may be written in the form

$$\frac{\delta\rho_{xx}}{\rho_{xx}}=\sum_{n=1}^{\infty}\frac{1}{2}\left(\frac{eV_n}{E_F}\right)^2\left(\frac{nl^2}{LR_c}\right)\left[1+\sin\left(\frac{4\pi nR_c}{L}\right)\right]. \quad (1)$$

In Eq. (1), the left hand side represents the fractional change in longitudinal resistivity due to the presence of COs, V_n is the potential amplitude of the nth harmonic component of the potential in the plane of the 2DEG, E_F is the Fermi energy, and R_c is the cyclotron radius of the electron orbits. Minima in the fundamental component of the COs are predicted to occur when

$$R_c=\frac{L}{8}(4k-1), \quad (2)$$

where k is the index of the CO (an integer). Our standard procedure for estimating the amplitude of the fundamental potential component V_1 is to determine the amplitude of the resistivity oscillation at a particular k, using two resistance maxima and the minimum in between and substitute in Eq. (1), choosing appropriate values for the 2DEG parameters at the field corresponding to the minimum. This procedure allows approximately for the effect of a linear background magnetoresistance variation and for the damping. It also suppresses the contribution from any second harmonic in the potential. (As we shall see, the second harmonic contribution to the COs is usually the most important after the fundamental.) In an alternative approach, which eliminates completely the effect of a linear background, the magnetoresistance trace is numerically differentiated and fitted with a derivative form of Eq. (1).

The R_c term in the denominator of Eq. (1) implies that the amplitude of the COs drops in direct proportion to the magnetic field with increasing k. In practice, this behavior is rarely observed, as has been pointed out by several authors.[15,16] Representative data, obtained using the derivative method, are plotted in Fig. 1(a). In this figure, the measurement made in the dark hardly shows any region of linearly decreasing amplitude but after illumination with a red light emitting diode and subsequent study again in the dark [dark after light (DAL) data], the transport mean free path is approximately doubled and a linear region clearly emerges. The vertical bars on Fig. 1(a) correspond to fields at which circumference of the cyclotron orbit is equal to the appropriate transport mean free paths. Clearly the COs are attenuated at much higher fields. If we look at the more complete solution of the Boltzmann equation for a single relaxation time also described by Beenakker,[5] and further refined by Menne and Gerhardts,[19] then it can be shown that, in the limits $R_c > L$ and $R_c \sim l$, the amplitude of the COs is multiplied by an additional Dingle factor $\pi R_c/l \sinh(\pi R_c/l)$, which leads to attenuation of the oscillations when an electron cannot describe a cyclotron orbit without scattering. In Fig. 1(b) we fit the data using this functional form. Two things should be noted about the fits. First as described above, reasonable agreement can only be achieved by using a mean free path l_{CO} very much shorter than the transport mean free path. For all data sets, l_{CO} is intermediate between the quantum mean free path l_q and the transport mean free path, as illustrated by the fitting magnetic field parameters for Fig. 1(b) given in its caption. Bøggild *et al.*[15] have also shown by means of simulations that the effective mean free path for smearing of the COs is less than the transport mean free path (by factors of 1.6 and 3.75 in the simulations reported) which they ascribed to the more important role of small angle scattering in degradation of the COs than in transport. It is interesting to note though that in our Dingle fits, much smaller effective mean free paths need to be assumed than are implied by these simulations. Secondly, although the Dingle factor fits give a reasonable first order approximation to the observed behavior, they do not predict a sufficiently rapid decay of amplitude at small fields. This has also been noted in a recent discussion of this problem by Paltiel *et al.*[16] These authors introduced a model for the scattering which suggested a $B\exp[-(B_0/B)^3]$ dependence for the CO amplitudes. Fits of this type are also included in Fig. 1(b). Both the dark and the DAL data are satisfactorily fitted using this function with values of B_0 of 0.16 and 0.12 T. These are similar in magnitude to those found by Paltiel *et al.*

In order to use the amplitude of the COs to deduce the modulation potentials, one would ideally like to make an allowance for the scattering. In principle one could make a fit to the amplitudes at high k to deduce B_0 and correct the raw amplitudes accordingly. In practice, however, there are rarely enough oscillations observed to perform such a correction reliably, particularly when the potential is strong and the PMR structure is prominent. The alternative procedure, esti-

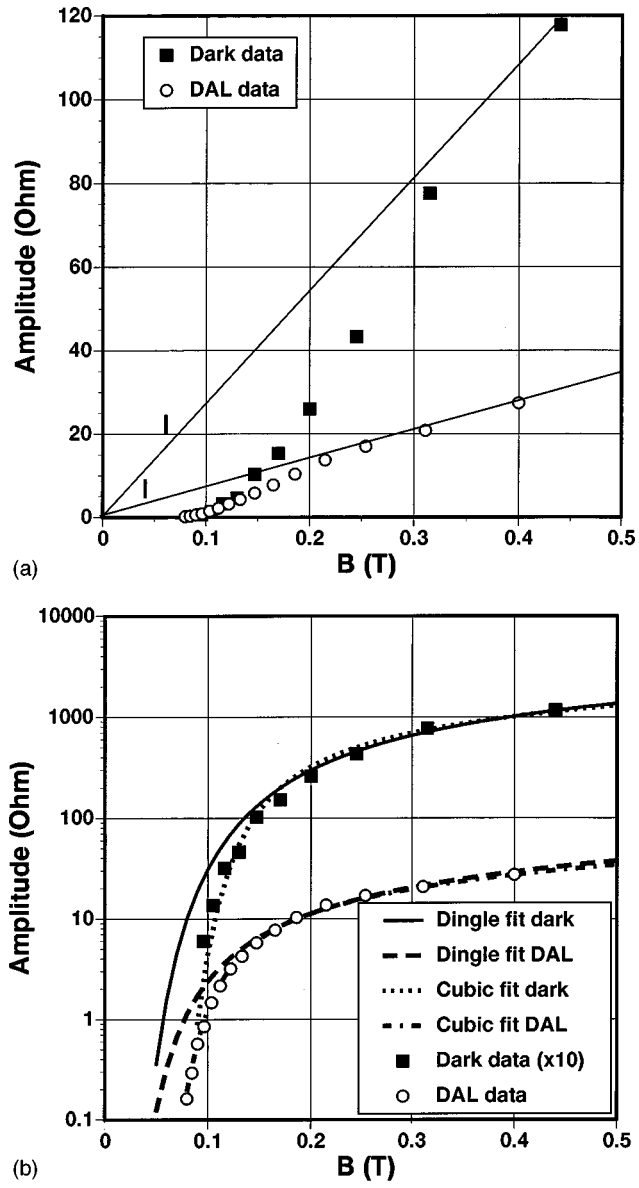

FIG. 1. (a) Amplitudes of COs for a type 3 sample in the dark and after illumination (DAL). The period of the superlattice was 300 nm. It was measured without bias applied to the gate, so that the COs result from strain effects. The lines drawn are to guide the eye to the linear region of the characteristic. The vertical bars mark the fields at which the circumferences of the cyclotron orbits are equal to the transport mean free paths (0.064 and 0.041 T, respectively). The corresponding values for the quantum mean free paths are 2.4 and 3.0 T. (b) Fits to the data of (a) the Dingle factor fits use equivalent magnetic fields (fields at which the mean free path is equal to half the circumference of the cyclotron orbit) of 0.45 and 0.30 T for dark and DAL data, and the cubic fits have $B_0 = 0.16,\ 0.12$ T. The dark data is offset by a factor of 10 for clarity.

mating B_0 from the known mean free paths, is not possible because of the empirical component in the theory. A recent calculation by Mirlin and Wolfe[20] confirms the empirical relation of Paltiel *et al.* and includes an explicit expression for the parameter B_0. However, the values calculated from this expression are between 2 and 3 times larger than we observe experimentally and do not differ significantly for dark and DAL data. We are thus unable to use this expression reliably to calculate values of B_0 to correct our data. Our procedure therefore is to use uncorrected amplitude data to evaluate the potentials from Eq. (1). We use the lowest k oscillation where the data is not confused by the overlying Shubnikov–de Haas oscillations (typically $k=2$) and for comparative work on the same sample at different gate biases, we are careful to stick to the same oscillation as far as possible. It should always be born in mind, however, that the potential values we quote may be systematically reduced by the effects of scattering. We discuss the magnitude of this reduction in Sec. III D below when we have evaluated other means of determining the periodic potential.

B. Harmonic content of the COs

One of the most obvious features of the COs seen for long period superlattices deposited on shallow layers is that there are higher harmonics than the first present in the traces. The harmonic content provides important information about the origin of the modulation and hence it is critical to determine it as accurately as possible. A qualitative indication of the harmonics present can be obtained by Fourier transforming the magnetoresistance data. However, because of problems with windowing and with allowing correctly for the amplitude of the oscillations falling with increasing k, we prefer to determine the harmonic content by reconstructing the magnetoresistance oscillations using Eq. (1). An example of such a reconstruction including first, second and third harmonics is given in Fig. 2. We estimate the accuracy with which the higher harmonic components are determined in this case is $\pm 20\%$. One other point about this figure should be noted. The field values of the extrema of the experimental trace are reproduced to within 2% by the reconstruction. This is consistent with the probable error in the superlattice period resulting from the calibration of the electron beam pattern generator (better than $\pm 3\%$). However, if the extrema of the fundamental component are calculated, these do not correspond accurately to any structure in the observed COs (see Fig. 2). Hence, when the traces contain a high harmonic content, it is inaccurate to try to deduce the period of the LSSL from such extrema. This point has also been discussed in a recent paper by Paltiel *et al.*[21] who came to similar conclusions.

C. The low field positive magnetoresistance step

A prominent feature of the magnetoresistance data obtained for LSSLs with reasonably strong modulation is the PMR ''step'' which occurs at low fields, below the COs. This was explained by Beton *et al.*[7,8] in terms of lateral electron streaming orbits which are dominant at low magnetic fields but are no longer possible when the Lorentz force on an electron at the Fermi level due to the applied magnetic field exceeds the maximum force resulting from the periodic electrostatic field, the region of magnetic breakdown. For a simple sinusoidal potential without harmonics, the upper critical field for streaming orbits is given by

$$B_c = \frac{\mathcal{E}_{\max}}{v_F} = \frac{2\pi V_1}{L v_F}, \tag{3}$$

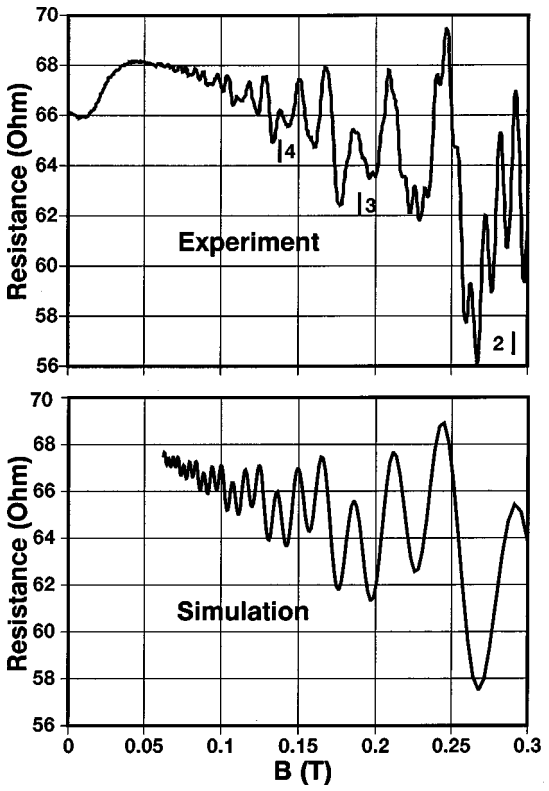

FIG. 2. The simulated magnetoresistance for a 400 nm period LSSL fabricated on a type 1 material compared with the magnetoresistance measured at 4.2 K. Fitting parameters: $V_1=0.34$ meV, $V_2=0.11$ meV, $V_3=0.26$ meV. The vertical bars correspond to the minima of the fundamental component of the COs. At higher fields the experimental data is overlain by Shubnikov–de Haas oscillations.

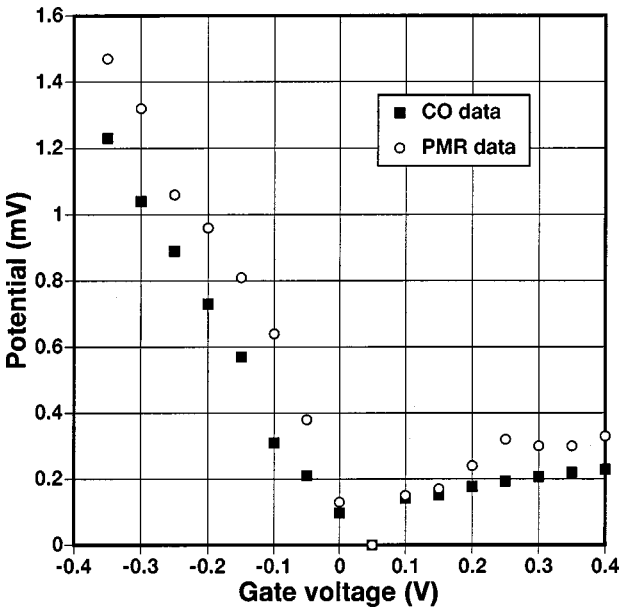

FIG. 3. Comparison of fundamental potentials deduced from the CO amplitudes and the low field PMR step. The sample was a 200 nm superlattice deposited on a type 2 layer and had no detectable second harmonic component in the COs.

where $\mathcal{E}_{\max}$ is the maximum electric field in the system and v_F is the Fermi velocity. A more recent solution of the Boltzmann equation by Müller *et al.*[22] using a square rather than a sinusoidal potential can be used to reproduce the main features of this phenomenon and Eq. (3) with different numerical constants. Although the arguments of Beton *et al.* are restricted to a simple sinusoid, we have confirmed using simulations that in the case where multiple harmonics are present Eq. (3) applies provided that all the harmonics are considered in the calculation of $\mathcal{E}_{\max}$. Equation (3) may be combined with Eq. (2) to relate B_c to the field at the kth minimum of the COs, B_k

$$\frac{B_c}{B_k}=\frac{\pi}{8}\left(\frac{eV_1}{E_F}\right)(4k-1). \tag{4}$$

This equation gives a convenient method for estimating the magnitude of the potential without knowledge of the period of the LSSL, provided that it is harmonic free. It also confirms the important experimental result that, as the potential grows in strength, the number of COs clearly visible above the positive magnetoresistance step declines.

To use Eq. (3) in order to deduce the magnitude of the modulating potential, we need to decide where on the characteristic the point corresponding to the critical field lies. This process is complicated by the smooth nature of the transition from the step into the COs. Whereas the theories[7,22] suggest that the additional contribution to the resistance should drop to zero at B_c, what is observed generally is a flattening out of the magnetoresistance trace and a smooth transition into the region of the COs. In the absence of a clearly defined experimental measure of B_c, we project the steepest slope on the step to the peak value and define the critical point to lie there. However, this procedure introduces considerable systematic uncertainty in the value of the potential deduced, which we estimate to be of the order of $\pm 20\%$.

The magnitude of the PMR step also depends (roughly quadratically) on the strength of the periodic potential. However, it is difficult to develop reliable relations for interpreting this data and so we do not discuss this further.

D. Comparison of different techniques for deducing potentials

In Fig. 3, we compare magnitudes of the modulation potential deduced from CO amplitudes and from the PMR step for various gate voltages. The sample consisted of a 200 nm LSSL on a type 2 layer, which was especially chosen because it showed no evidence of any second harmonic component in the COs. The two sets of data are qualitatively in excellent agreement, showing a steep rise at negative bias, a zero of potential offset with respect to the gate voltage zero and an increase and saturation at positive gate voltage. These features will be discussed in detail in the next section. Of more importance here is the ratio between the potentials deduced by the two techniques, which varies only between about 1.2 and 1.5 over the complete bias range (except near zero gate bias where the magnitudes are small and the errors are large), with the value deduced from the PMR being higher. We are unable to account unambiguously for this high ratio, but provisionally we attribute it primarily to the difficulty in judging the field at the true PMR peak as dis-

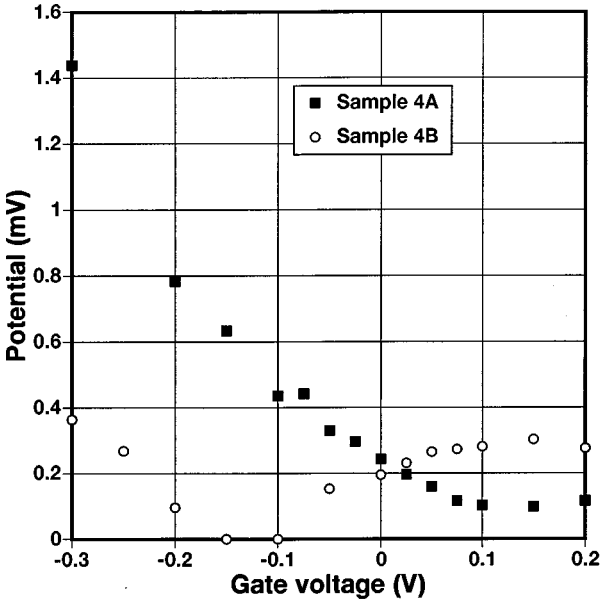

FIG. 4. Modulation potentials for two 300 nm superlattices on type 3 material. Sample 4A was aligned so that the current flowed along $[01\bar{1}]$ and sample 4B was aligned so that the current flowed along [011].

cussed above. It is unlikely to arise from any underestimate of V_1 from the CO amplitudes resulting from the effects of scattering because there is no apparent tendency for the ratio to decrease at large negative biases, where the mean free paths are short and these effects are expected to attenuate the amplitude of the COs most severely. The good agreement between potential modulation values deduced from these two different measurements generates confidence that we can reliably deduce the modulating potentials over a wide range of biases. Similarly good agreement has also been reported by Paltiel *et al.*[21] and by Emeleus *et al.*[23] for samples modulated by surface etching which contain only a fundamental component in the COs.

In samples with a higher harmonic content in the COs such as that shown in Fig. 4, the position of the PMR step leads to even higher values for the effective potential, particularly where the fundamental component is small.[23] This is expected because the higher harmonics can give rise to large contributions to the maximum electric field. Hence our overall judgment is that, although the PMR step can give a good guide as to the general magnitude of the first harmonic of the potential, it generally overestimates it, and that more reliable data can be obtained from the amplitude of the COs at small k.

IV. COMPARISON OF EXPERIMENTAL OBSERVATIONS WITH THEORETICAL CALCULATIONS

A. General behavior of the potential modulation with gate bias

The data of Figs. 3 and 4 shows clearly the main features we observe in all our samples, and which we may summarize as follows: A nonzero potential modulation in the absence of gate bias, A minimum in potential modulation at a gate voltage offset from zero, An approximately linear increase of modulation amplitude with gate voltage at the negative side of the minimum, A tendency for the modulation amplitude to saturate towards a constant value at the positive side of the minimum.

We explained these features of the characteristic qualitatively in our previous publication,[14] which was based on a study of type 2 samples. At zero bias we postulate that only the strain modulation is acting. As gate voltage is applied, an electrostatic modulation develops and, depending on the sign of the piezoelectric modulation, either adds to or subtracts from it. In one bias direction therefore the overall potential increases, and in the other it reaches a minimum before increasing again. We pointed out that for samples aligned so that the current flowed along [011] the piezoelectric coupling was predicted to be a maximum and of opposite sign to that expected for a current flowing along the $[01\bar{1}]$ direction, and reported that this prediction is born out convincingly in practice. The sample of Fig. 3 (sample 2 of Ref. 14) was aligned with a current flow direction at 30° to $[01\bar{1}]$, and hence has a slight offset of the minimum to positive gate voltage values.

In Fig. 4 we show data from an equivalent experiment on a type 3 layer. Two samples were studied, with current flowing in the [011] and $[01\bar{1}]$ directions, respectively. Once again we observe the characteristic asymmetry in the data for the two orientations, with minima at opposite sides of zero bias. The offsets are of the same sign as reported in our previous work, but the minima occur at about ± 0.15 V, rather than ± 0.05 V observed typically in the type 2 samples with similar superlattice periods. We ascribe this difference primarily to the greater depth of the type 3 layer. The electrostatic modulation decays monotonically with depth,[11] whereas the fundamental of the piezoelectrically mediated strain modulation increases until $L/d \approx 2.5$ before decreasing again (see below). Taken together these results imply that a greater electrostatic potential is required to annul the piezoelectric contributions.

Using the data from Ref. 14 and from Fig. 4, together with the obvious result that a negative potential under the gates will produce a negative potential (positive potential energy) for electrons beneath, we can deduce the sign of the potential introduced by the piezoelectric effect resulting from strain under metal gates. We find that for current flowing in the $[01\bar{1}]$ direction (samples 1B and 4A), the piezoelectric potential is positive under the gates, and vice versa for the [011] samples. Larkin *et al.*[13] have calculated the potential assuming that the metal gates do not stress the semiconductor beneath when they are deposited, and that the strain develops due to differential thermal contraction as the sample is cooled. They predict, however, *the opposite sign of perturbation* from that which we observe. We therefore conclude that our hypothesis that when deposited the gates are unstrained is incorrect and that there is sufficient intrinsic compressive strain after deposition to dominate the effect of thermal contraction.

The asymmetry between the two different directions for current flow which we report here for a type 3 layer and in Ref. 14 for type 2, is also seen in the type 1 samples, though there the behavior is complicated by the parasitic layer of electrons screening the channel from the gates, which has to

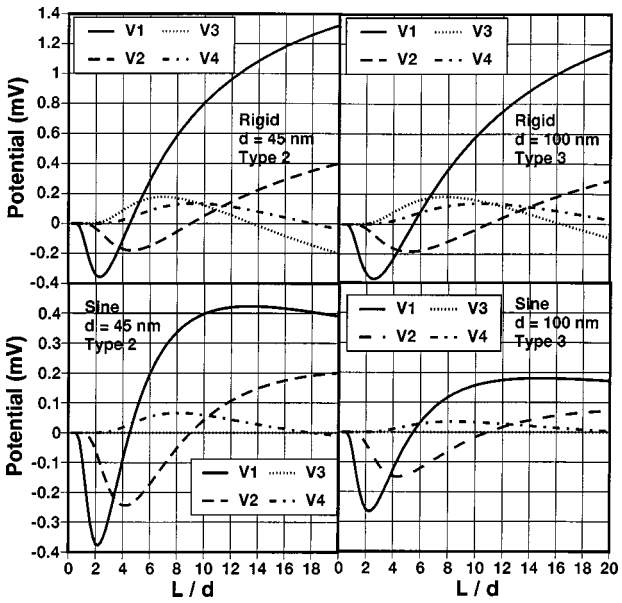

FIG. 5. Theoretical plots of first four Fourier components of the potential as a function of normalized superlattice period predicted for piezoelectric coupling using two models from Ref. 13. Layer parameters are for type 2 and type 3 samples.

be removed by negative bias before the potential of the gates can affect the channel.[10] All the remaining data discussed in this paper are for samples aligned parallel to the $\langle 011 \rangle$ cleavage directions, and hence concerns the fully developed piezoelectric modulation. We shall henceforth ignore questions of the absolute sign of the potential and concentrate on the magnitude of the piezoelectrically generated modulation.

B. Modulation at zero gate bias—magnitude and harmonic content

The modulation at zero gate bias represents then the effect of the elastic strain piezoelectrically coupled to the 2DEG. The magnitude of this modulation has been calculated by Larkin *et al.*,[13] assuming as discussed above, that the strain results from differential thermal contraction between the gate and the heterostructure during cooling and has an appropriate magnitude. Some representative results from these calculations are shown in Fig. 5. These plots give the predicted amplitudes for the first four harmonics of the potential as a function of the ratio of superlattice period to 2DEG depth (L/d), and are for superlattices with equal mark/space ratios. The depth parameters are appropriate for type 2 and type 3 samples. Calculations are shown for two simple elastic models of gate behavior. The first, the rigid gate model, assumes a constant lateral stress under the gates, which leads to a concentration of force on the semiconductor at the their edges. In the second, the sine force model, the force is distributed across the gates sinusoidally, and is not singular at the edges. The strengths and weaknesses of these models are discussed in Ref. 13. All the calculations assume screening by a charge layer around the donors or at the boundary of the spacer, where the donors nearest to the channel are situated, respectively. As explained by Larkin *et al.*, it is most plausible to assume such screening, as the piezoelectric modulation will be almost fully established at temperatures above 150 K before the DX centers in the layers freeze and further screening by the donor layer becomes impossible.

The diagrams show clearly the main features of the calculations, which are common to all.

(i) The potential components increase from zero at zero period. At small periods, the first harmonic of the potential is dominant.

(ii) The form of the potential curves is similar for different depths of the 2DEG, when plotted versus L/d. This behavior is readily seen in the curves for the type 2 and type 3 samples in Fig. 5. It is only accurate if screening by the intermediate donor layer is ignored, but is approximately correct even if this screening is included.

(iii) As the period increases, all the harmonics pass through zero and change sign. The periods at which they do so are proportional to the index of the harmonic.

(iv) At large periods, the first harmonic is dominant, with an appreciable content also from the second harmonic. The higher harmonics are somewhat lower in amplitude.

(v) For the sine gate model, at unity mark/space ratio, the third harmonic is identically zero. The first harmonic saturates at a period which depends on the thickness of the gates and the elastic constants which are assumed.

Most of these features are seen at least qualitatively in the data. In Fig. 6 we plot the magnitudes of the potentials observed for a range of samples of all types as a function of the ratio of period to 2DEG depth (L/d). This form of abscissa is adopted to test the similarity noted above. The amplitudes of the fundamentals for type 1 samples (for which the data covers the fullest range) are plotted in Fig. 6(a), and in Fig. 6(b) the equivalent data for the type 2 and 3 samples is presented. The amplitudes of all the harmonics detected for the type 1 samples (for which the most exhaustive study has been made) are given in Fig. 6(c). In all these figures relevant theoretical curves are included, to aid comparison with experiment. These were calculated for an assumed strain in the gate of 0.001 (derived by Davies and Larkin[11] from thermal expansion arguments). No account is taken either in the theoretical plots or in the data of the signs of the potentials, which are in any case not known for the majority of the type 1 samples. All the data shown is for samples with nominally equal mark/space ratios, to which the theoretical curves in Fig. 5 apply. The type 1 superlattices include one with a period of 60 nm, which we believe to be the smallest period fully gateable lateral superlattice yet reported. Its behavior was completely in line with the classical models used to analyze the data for larger period samples; no signs of any behavior associated with possible quantum effects were seen.

We discuss first the type 1 samples in Fig. 6(a). Although the data is a little scattered, all the features noted above can be distinguished. The magnitude of the potential modulation rises from low values at short periods, shows a maximum at around $L/d=2.5$, and then declines to small values again at around $L/d=5$. For longer periods, larger values of the potential are again observed. As noted in the theoretical discussion of the piezoelectric coupling,[13] the predicted magnitude of the first harmonic is in reasonable agreement with the experiments,[9,10] though there are some samples for which the assumed strain is too low. Thus although the evidence from the directional experiments is that the differential thermal contraction model for the strain does not predict the correct

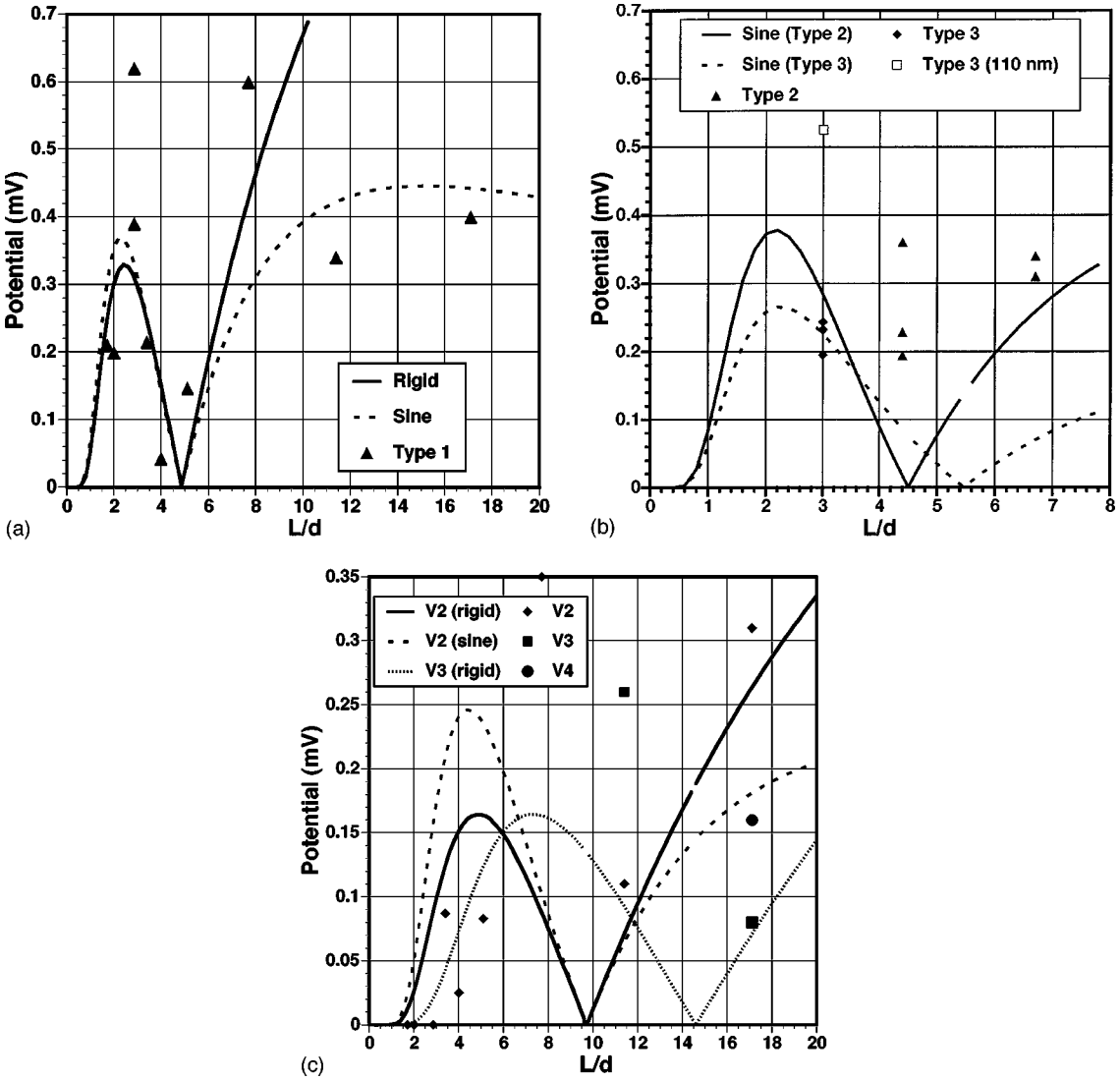

FIG. 6. (a) Experimental values for magnitude of the first harmonic of the potential for samples of type 1 plotted against normalized superlattice period. The superimposed theoretical curves are for different models for the elastic strain. (b) Magnitude of the first harmonic of the potential for type 2 and type 3 samples, compared with theoretical curves for the sine model. All gates were 25–30 nm thick apart from the thick gate sample marked which had a 110 nm gate. (c) Magnitudes of higher harmonic components of the potential as a function of normalized period. All data and theory is for type 1 samples. Note that for the sine model, the third harmonic is predicted to have zero amplitude.

sign (see above), it does predict effects of the correct magnitude. The experimental scatter is likely to result from variations in the strain built into the sample during deposition. The long period data is too scattered to enable us to distinguish between the ''rigid'' and ''sine'' models. Passing on to Fig. 6(b), the data is too restricted in range of L/d to enable the same features as in the type 1 data to be distinguished. However the modulation magnitudes are similar to those plotted in to Fig. 6(a), as expected. Moreover groups of samples of the same period generally have similar potential modulations, which is a good indication of the consistency of the data. One deviation from this general observation is worthy of note. It concerns the sample marked type 3 (110 nm) which was specially fabricated with a 110 nm thick gate, as opposed to the 25 or 30 nm used for all the other samples in Fig. 6. The magnetoresistance trace for this sample is compared in Fig. 7 with that for a sample identical apart from having a 25 nm gate. The resistances of the two samples are similar but the COs for the thicker gate structure are much stronger, which is reflected in the magnitude of the fundamental potential component which is 0.53 meV for the thick gate, and only 0.23 meV for the thinner one. This significant increase in the amplitude with gate thickness confirms the dominant role of strain in producing the modulation. A thicker gate is expected in certain cases to exert a larger strain on the underlying semiconductor[13] but not to change any electrostatic modulation of the 2DEG. It also suggests that the simple rigid gate model, where the strain induced is independent of the thickness of the gate is too simple, and that a more sophisticated model would be necessary to explain the data fully.

We now pass on to discuss the harmonic data in Fig. 6(c), which is overlaid with the predictions for the second and third harmonics for the rigid and sine gate models. Although

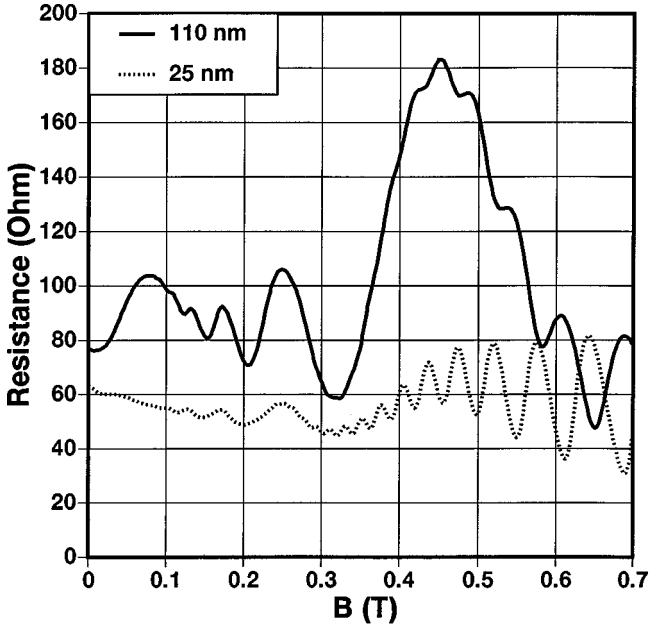

FIG. 7. Magnetoresistance traces for two 300 nm period samples with different gate thicknesses deposited on the same type 3 layer and measured at 1.4 K.

the data is sparser than for the first harmonic, the trends suggested by theory are indeed observed. At small L/d, COs with only first harmonic content are seen. This absence of higher harmonics at small periods is in agreement with the predictions of the piezoelectric models (although it should be pointed out that in any coupling mechanism the higher harmonics decay more rapidly at short periods than the fundamental). At around $L/d=3$, second harmonic components begin to be seen in the data, and these remain significant over much of the rest of the range. It was this strong second harmonic component which led us initially to examine the effect of strain from periodic gates in modulating the 2DEGs in these heterostructures. Although a weak second harmonic component is predicted[11] for electrostatic modulation under certain circumstances even for a mark/space ratio of unity, the strength of the second harmonic observed is far greater than anticipated from this source.[11] It is, however, of similar magnitude to that predicted by the piezoelectric model. Of course real gate patterns never have precisely unity mark/space ratios in practice, but an error of ± 5 nm in a 200 nm LSSL with a nominally 100 nm gate, the maximum suggested by the inspection of the superlattices in a high resolution scanning electron microscope, would only lead to an additional second harmonic component of around 4% of the first, much less than is generally observed. Our study of second harmonic structure confirms therefore the behavior is qualitatively as expected for strain coupled piezoelectrically to the 2DEG. Quantitatively, however, the second harmonic data is rather scattered and there is insufficient data to support the existence of the predicted minimum of the second harmonic component at $L/d\approx 10$.

The main discrepancy between theory and experiment in the harmonic data is that third (and fourth) harmonic components have only been detected in the data at L/d ratios above 10, as illustrated in Fig. 6(c). The rigid gate model predicts that they should be observed at smaller periods, whereas in the sine model zero third harmonic is predicted. This suggests that neither of these models fully describes the data. One additional factor should also be taken into account in considering this observation, however. The higher harmonics in the potential are strongly influenced by behavior at the edges of the gate,[13] and it is well known that the final stage in the LSSL fabrication process, the lift-off procedure, can cause varying amounts of lifting and curling of the gates at their extremities. Such an effect is liable to produce large variations in the harmonic components from sample to sample.

In two recent experiments,[23,24] potential modulation of a GaAs/AlGaAs 2DEG by a pseudomorphic heteroepitaxial InGaAs layer has been reported. Both these papers report harmonic content in the COs. Emeleus *et al.*[23] working at an effective L/d ratio of around 7 and samples of unity mark/space ratio, observed a strong second harmonic component in the modulation in the piezoelectrically active directions, but do not report any higher harmonics. This data is broadly in agreement with that summarized above for the metal gated samples. Although a detectable third harmonic might be expected in this data, it was not observed. Luyken *et al.* on the other hand use longer periods with $L/d\approx 12$, and see a potential containing strong harmonics up to the sixth. Unfortunately their samples had mark/space ratios very different from 1, and so their data cannot be compared directly with the observations in this paper.

C. Behavior at negative gate bias

We now move on to discuss how the potential under the superlattice varies with gate bias. We assume that the piezoelectric contribution to the potential is independent of bias and therefore that any bias dependence reflects the change in the electrostatic contribution to the potential alone. This is expected in principle (the different contributions act independently) and was confirmed by Skuras *et al.*[14] who showed that the second harmonic contribution to the potential, derived overwhelmingly from the piezoelectric interaction, was independent of bias on the sample. Looking first at the behavior in negative bias, we see, for type 2 and type 3 samples, a potential which increases in magnitude roughly linearly with bias (Ref. 14 and Figs. 3 and 4). The other significant observation from the COs in this bias range is that the minima move to lower magnetic fields as the bias is made more negative, reflecting the decrease in mean carrier concentration. Analysis of this data assuming Eq. (1) enables us to deduce how this mean carrier concentration beneath the LSSLs varies with bias. Some data are given in Fig. 8 and in Table I. Although taken from the positions of the CO minima, they are confirmed by analysis of Shubnikov–de Haas oscillations from the region beneath the gates. The type 3 samples deplete linearly with negative bias, with the linear fit to the data intersecting the axis at an effective bias voltage of around -0.7 V. This behavior is predicted by the simple electrostatic models.[11] For a mark/space ratio of unity, and a pinned free surface (fixed Fermi level), the mean potential at the 2DEG is predicted to be exactly one half that for a continuous gate biased to the same potential and for a frozen free surface (constant charge density at low temperatures) the predicted result is also close to a half. Therefore in the linear region the gradient dn/dV_g will be half that predicted for the

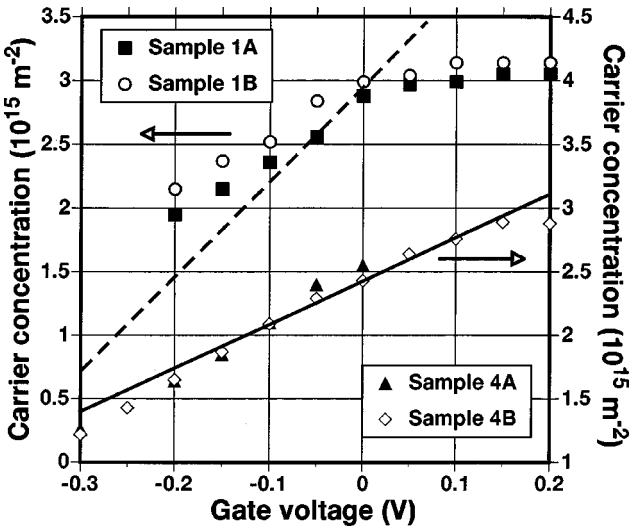

FIG. 8. Mean carrier concentrations as a function of gate bias for type 2 samples (1A and 1B: left hand ordinate) and type 3 samples (4A and 4B: right hand ordinate). Solid line: predicted variation under negative bias for type 3 samples. Hatched line: predicted variation for type 2 samples.

continuous gate. The solid line drawn in Fig. 8 is as predicted for a type 3 sample from the gate capacitance and is in reasonable agreement with experiment. This demonstrates conclusively that there is no tendency for charge movement, either on the surface of these LSSLs or in the donor layer, under the action of the lateral electric field induced by the gates to screen their potential. For the type 2 samples on the other hand, the depletion data is strongly affected by the presence of a low concentration of electrons in shallow states in the donor layer, which can be removed by the application of bias and affect the rate of depletion. Around zero bias therefore the rate of depletion in these samples is much lower than the capacitance calculation (hatched line) predicts. This difference in behavior is also evident in the numerical values for dn/dV_g given in Table I. Similar reductions in the rate of accumulation can of course be seen for all samples in positive bias, where electrons are induced in shallow states round the donors.

We now examine the behavior of the first harmonic of the periodic electrostatic potential of the gates as determined from the amplitudes of the COs. The limiting electrostatic contribution can be estimated by the value of dV_1/dV_g, the rate of change of modulation potential with gate voltage, in the limit of large negative bias; theoretical and experimental values for this quantity are also included in Table I. Two theoretical calculations are given, one including the screening not only by the channel electrons but by the parasitic layer round the donors, and the other omitting the latter. Starting with the type 2 samples, where the piezoelectric contribution is relatively small, agreement between experimental and theoretical values including screening by the donors is quite reasonable. This is as expected given that some screening by the donor layer is evident in the carrier density data. For type 3 samples, the data (see Fig. 4) is less clear because of the larger piezoelectric modulation, but in the limit of strong negative bias, for the $[01\bar{1}]$ sample (4A), the experimental value is well above that predicted for donor layer screening and approaches the unscreened value, as expected. We conclude that in negative bias the electrostatic perturbations are present and that their magnitudes are calculable using the models of Davies and Larkin[11] to an accuracy of better than $\pm 50\%$, provided that the correct screening terms are included.

D. Behavior at positive gate bias

At positive gate bias, Figs. 3 and 4 both show that the amplitude of the first harmonic of the perturbation begins to change less rapidly than at negative gate bias and indeed to saturate. This behavior is associated with a tendency for electrons to flood into shallow states in the donor region, and to screen the channel from the gate potential, so that the density of channel electrons generally does not increase greatly over that present at zero bias (see Fig. 8). We believe that the reason for the saturation of the periodic potential is similar, screening by electrons in the donor layer. However, this hypothesis suffers from one immediate problem. As explained in the preceding section, we have already included in our analysis of the behavior of type 2 samples a measure of

TABLE I. The rate of variation of the mean carrier concentration and modulation potential with gate bias for various samples on type 2 and type 3 layers compared with theory. Data taken in the limit of strong negative bias. For theoretical models used, see text.

Sample	Type	Period (nm)	dn/dV_g (Expt.) $\times 10^{15}$ m^2 V^{-1}	dn/dV_g (Theory) $\times 10^{15}$ m^2 V^{-1}	dV_1/dV_g (Expt.)	dV_1/dV_g (Theory) (screened)[b]	dV_1/dV_g (Theory) (not screened)[b]
1A	2	300	4.2	7.6	0.0075	0.011	0.055
1B	2	300	4.2	7.6	0.0065	0.011	0.055
2	2	200	2.2	7.6	0.004[a]	0.0095	0.044
3A	2	200	7	7.6	0.004[a]	0.0095	0.044
3B	2	200	3.0	7.6	0.003[a]	0.0095	0.044
4A	3	300	4.2	3.4	0.007	0.0019	0.015
4B	3	300	4.4	3.4	0.003	0.0019	0.015
5	3	300	4.1	3.4		0.0019	0.015

[a]Data taken from PMR step. For theoretical models used, see text.

[b]Screened and not screened refers to the effect of the doping layer.

screening in the donor layer, treating the parasitic electrons there as a 2DEG, which introduces a linear correction. But experiment shows that the screening is increasing in efficiency as one passes into positive bias. We believe that the reason for this is that our hypothesis that the donors screen as a 2DEG breaks down at positive bias due to the rapidly widening potential well (and possibly also to some spreading of the donor layer). However, we do not have a quantitative theory for this behavior. In type 3 samples, a broad potential well at the boundary of the dopant slab emerges naturally at positive bias,[25] and this three-dimensional screening picture is the natural one to apply.

V. CONCLUSIONS

In this paper, we have shown that the magnitudes of the commensurability oscillations are broadly in agreement with our theoretical analyses of the piezoelectric and electrostatic contributions to the potential modulation, for three different layer structures and a wide range of superlattice periods. Such discrepancies between theory and experiment as are still found, can be ascribed either to detailed differences in layer properties, notably in screening by the donor layers, or to likely variations in strain in the gates, particularly at their edges, which are likely to result from unavoidable fluctuations in deposition conditions. The incorporation of intentionally stressed layers in lateral superlattice samples is likely to offer a route to intense periodic modulations at short periods.

ACKNOWLEDGMENTS

This work was supported by the U.K. EPSRC. J.H.D. was financially supported by the Leverhulme Trust (U.K.) and by QUEST, a National Science Foundation Science and Technology Center, Grant No. DMR 91–20007.

*Electronic address:arlong@elec.gla.ac.uk

†Present address: Department of Physics, Sheffield University, Sheffield, S3 7RH, U. K.

[1] C. W. J. Beenakker and H. van Houten, *Solid State Physics*, edited by H. Ehrenreich and D. Turnbull (Academic Press, Boston, 1991), Vol. 44, p. 1.

[2] D. Weiss, K. von Klitzing, K. Ploog, and G. Weimann, Europhys. Lett. **8**, 179 (1989).

[3] R. R. Gerhardts, D. Weiss, and K. von Klitzing, Phys. Rev. Lett. **62**, 1173 (1989).

[4] R. W. Winkler, J. P. Kotthaus, and K. Ploog, Phys. Rev. Lett. **62**, 1177 (1989).

[5] C. W. J. Beenakker, Phys. Rev. Lett. **62**, 2020 (1989).

[6] R. R. Gerhardts, Phys. Rev. B **45**, 3449 (1992).

[7] P. Beton, E. S. Alves, P. C. Main, L. Eaves, M. W. Dellow, M. Henini, O. H. Hughes, S. P. Beaumont, and C. D. W. Wilkinson, Phys. Rev. B **42**, 9229 (1990).

[8] P. Beton, M. W. Dellow, P. C. Main, E. S. Alves, L. Eaves, S. P. Beaumont, and C. D. W. Wilkinson, Phys. Rev. B **43**, 9980 (1991).

[9] R. Cuscó, M. R. Holland, J. H. Davies, I. A. Larkin, E. Skuras, A. R. Long, and S. P. Beaumont, Surf. Sci. **305**, 643 (1994).

[10] R. Cuscó, E. Skuras, S. Vallis, M. C. Holland, A. R. Long, S. P. Beaumont, I. A. Larkin, and J. H. Davies, Superlattices Microstruct. **16**, 283 (1994).

[11] J. H. Davies and I. A. Larkin, Phys. Rev. B **49**, 4800 (1994).

[12] See, for example, P. D. Ye, D. Weiss, R. R. Gerhardts, K. von Klitzing, K. Eberl, H. Nickel, and C. T. Foxon, Semicond. Sci. Technol. **10**, 715 (1995).

[13] I. A. Larkin, J. H. Davies, A. R. Long, and R. Cuscó, Phys. Rev. B **56**, 15 242 (1998).

[14] E. Skuras, A. R. Long, I. A. Larkin, J. H. Davies, and M. C. Holland, Appl. Phys. Lett. **70**, 871 (1997).

[15] P. Bøggild, A. Boisen, K. Birkelund, C. B. Sørensen, R. Taboryski, and P. E. Lindelof, Phys. Rev. B **51**, 7333 (1995).

[16] Y. Paltiel, U. Merav, D. Mahalu, and H. Shtrikman, Phys. Rev. B **56**, 6416 (1997).

[17] E. Skuras, M. C. Holland, C. J. Barton, J. H. Davies, and A. R. Long, Semicond. Sci. Technol. **10**, 922 (1995).

[18] A. K. Geim, R. Taboryski, A. Kristensen, S. V. Dubonos, and P. E. Lindelof, Phys. Rev. B **46**, 4324 (1992).

[19] R. Menne and R. R. Gerhardts, Phys. Rev. B **57**, 1707 (1998).

[20] A. D. Mirlin and P. Wölfe, cond-mat/9802288, 1998 (unpublished).

[21] Y. Paltiel, D. Mahalu, H. Shtrikman, G. Bunin, and U. Meirav, Semicond. Sci. Technol. **12**, 987 (1997).

[22] G. Müller, P. Středa, D. Weiss, K. von Kllitzing, and G. Weimann, Phys. Rev. B **50**, 8938 (1994).

[23] C. J. Emeleus, B. Milton, A. R. Long, J. H. Davies, D. Petticrew, and M. C. Holland, Appl. Phys. Lett. **73**, 1412 (1998).

[24] R. J. Luyken, A. Lorke, A. M. Song, M. Streibl, J. P. Kotthaus, C. Kadow, J. H. English, and A. C. Gossard, Appl. Phys. Lett. **73**, 1110 (1998).

[25] A. R. Long, J. H. Davies, M. Kinsler, S. Vallis, and M. C. Holland, Semicond. Sci. Technol. **8**, 1581 (1993).